Research Square

Preprints are preliminary reports that have not undergone peer review.
They should not be considered conclusive, used to inform clinical practice,
or referenced by the media as validated information.

Next generation nano-biocatalysts: Extremozyme-based nanoparticle system for Cypermethrin bioremediation

Juhi Barot
Naran Lala College of Professional and Applied Sciences
Nafisa Patel
nafisapatel@naralalacollege.edu.in
Naran Lala College of Professional and Applied Sciences
Vimal Prajapati
Navsari Agriculture University

Research Article

Keywords: Extremozyme, Laccase, Cypermethrin, PBD, CCD-RSM, Biogenic selenium nanoparticles, Bioremediation

Posted Date: July 13th, 2026

DOI: https://doi.org/10.21203/rs.3.rs-10086807/v1

License: This work is licensed under a Creative Commons Attribution 4.0 International License. Read Full License

Additional Declarations: No competing interests reported.

Version of Record: A version of this preprint was published at Applied Microbiology and Biotechnology on October 17th, 2026. See the published version at https://doi.org/10.1007/s00253-026-14053-z.

Abstract

Extremozymes, with their exceptional catalytic activity and stability under extreme environmental conditions, have great potential for pesticide remediation. This study involves the isolation and screening of a new extremozyme-producing microbe, *Proteus mirabilis* JB1, for the production of alkaline-pH-stable laccase. A primary OFAT screening tested a broad range of carbon sources (glucose, lactose, xylose, sucrose, starch, glycerol, cellulose, trisodium citrate, sodium acetate), nitrogen sources (ammonium sulfate, sodium nitrate, urea, beef extract, peptone, casein, gelatin), salts (0.1 mM and 0.01 mM) such as $CuSO_4$, KCl, $ZnCl_2$, $MgCl_2$, $MnCl_2$, $NiCl_2$, NaCl, and $CaCl_2$, and pH levels (7–10). The highest enzyme activity of 0.999 U/ml was achieved using 0.25% (w/v) cellulose, 0.8% (w/v) urea, 0.1 mM MnCl2, MgSO4, CaCl2, NaCl, and KCl, and 0.01 mM CuSO4, FeSO4, and NiCl2 at pH 9 with good stability to surfactants (Tween 80, SDS), organic solvents (acetone, ethanol, methanol), and inhibitor (EDTA). PBD and CCD were then implemented to screen and optimize critical parameters—cellulose (1.5% w/v), urea (0.7% w/v), and $MgSO_4$ (0.05 mM)—to achieve an efficient increase in enzyme activity to 2.3 U/mL, demonstrating the strength and efficacy of the optimization process. Biogenic selenium nanoparticles (Bio-SeNPs) were fabricated and exhibited very high efficiency in pesticide degradation, achieving 100% degradation of cypermethrin without forming any toxic intermediates within 72 hr. This research has provided a comprehensive and replicable technique covering microbial isolation, enzyme optimization, fabrication of a nanobiocatalyst, and its application.

Key points

A novel isolate was employed for extremozyme laccase production.

Optimization increased the yield by 9.58-fold.

Bio-SeNPs were employed to degrade cypermethrin, achieving 100% degradation within 72 hr.

Introduction

Cypermethrin, a synthetic pyrethroid insecticide, is widely employed in agricultural and domestic pest control due to its high efficacy and broad-spectrum activity. However, its extensive use has led to significant environmental accumulation, particularly in soil and aquatic ecosystems (Jones, n.d.; Rehman et al., 2024). Cypermethrin is recognized for its persistence, low water solubility, and strong affinity for organic matter, which contributes to its bioaccumulation and toxicity in non-target organisms. Chronic exposure has been linked to neurotoxicity, endocrine disruption, and ecological imbalance, prompting urgent efforts to develop sustainable remediation strategies (Kansal et al., 2023). Bioremediation, which leverages the catalytic potential of microbial enzymes, offers a promising alternative to conventional physicochemical methods, which often suffer from high energy demands, incomplete degradation, and secondary pollution. Among the enzymes explored for pesticide degradation, laccase (EC 1.10.3.2) stands out for its broad substrate specificity, ability to oxidize a wide range of phenolic and non-phenolic compounds, and minimal cofactor requirements. Laccases have effectively degraded various environmental pollutants, including dyes, pharmaceuticals, and pesticides, making them attractive candidates for cypermethrin detoxification (Orlando et al., 2024; Rajendran et al., 2025). Despite their catalytic versatility, free laccase enzymes often exhibit limited operational stability under environmental conditions, including fluctuating pH and temperature, as well as the presence of organic solvents. To overcome the stability limitation, nanobiocatalyst systems have emerged as a powerful strategy to enhance enzyme performance (Fahim et al., 2025; Tan et al., 2023). Selenium nanoparticles (SeNPs), in particular, have attracted attention for their biocompatibility, antioxidant properties, and ability to interact with biomolecules (Garza-García et al., 2023; Raturi et al., 2025). SeNPs offer a green and scalable platform for enzyme immobilization when synthesized via biological routes (Bisht et al., 2022; Ibrahim et al., 2024).

Recent studies suggest that laccase-coated selenium nanoparticles (Lac@SeNPs) can synergistically combine the catalytic activity of laccase with the stability and surface functionality of SeNPs (Bisht et al., 2022). This hybrid system enhances enzyme stability and reusability while also improving substrate accessibility and electron transfer during degradation reactions (Ren et al., 2024; Xu et al., 2023). Moreover, the nanoscale interface facilitates better dispersion in contaminated matrices, thereby increasing the contact efficiency with hydrophobic pollutants, such as cypermethrin (Timmis, 2010). Although there is

great promise in using laccase-seeded selenium nanoparticles (Lac@SeNPs), reports on integrating microbial laccase production, SeNP generation, enzyme immobilization, and pesticide degradation are few. Their ability to fully detoxify pesticides without producing toxic intermediates remains unknown. Addressing this gap is essential for developing robust, field-deployable biocatalytic systems for environmental remediation. The present study aims to isolate and screen a microbial strain producing high-activity laccase, optimize laccase production using statistical approaches including one-factor-at-a-time (OFAT), Plackett–Burman design (PBD), and Central Composite Design (CCD); synthesize selenium nanoparticles via biological methods and conjugate them with purified laccase to form Lac@SeNPs; characterize the enzyme and nano biocatalyst using UV–Vis spectroscopy, and electron microscopy; and evaluate the degradation efficiency of free laccase, SeNPs, and Lac@SeNPs against cypermethrin under controlled conditions. This integrated approach aims to develop a stable, reusable, and eco-friendly nanobiocatalyst for the effective remediation of cypermethrin-contaminated environments.

Materials and Methods

Sample Collection and Preparation

Environmental samples were collected from five locations known for industrial and organic contamination to isolate potential laccase-producing microorganisms. The sampling sites included: Industrial effluent discharge points, biological sludge from wastewater treatment plants, Chemical sludge from industrial processing units, and Industrial contaminated soil zones (21.099795416306733, 72.98735113010757), agrowaste composting soil (20.924622842084553, 72.90838138566238). Approximately 100–200 g of solid samples and 100 mL of liquid effluent were collected in sterile containers, transported on ice, and processed within 24 hours (Oyedeji et al., 2025). The potential isolate, *Proteus mirabilis* JB1, was isolated from industrial chemical sludge and maintained at the microbiology department of Naran Lala College of Professional and Applied Sciences, Navsari, India. Also, the 16S rRNA sequence has been deposited in GenBank under accession number PQ160485 and will be available from the corresponding author upon request for research purposes.

Enrichment and Primary Screening for Laccase-Producing Microbial Strains

10 mL of each sample (10 g of soil/10 mL of sludge) was inoculated into 100 mL of Minimal Salt Medium (MSM) supplemented with 2 mM guaiacol as an indicator substrate and 0.5% (w/v) glucose as a carbon source for enrichment of laccase-producing microorganisms. The medium composition was as follows: K_2HPO_4 (0.173% w/v), KH_2PO_4 (0.0680% w/v), $MgSO_4.7H_2O$ (0.01% w/v), NaCl (0.4% w/v), $FeSO_4.7H_2O$ (0.003% w/v), $CaCl_2.2H_2O$ (0.002% w/v), $CuSO_4$ 0.2mM (Bibi et al., 2023). Cultures were incubated at 37 ± 1°C for 72 hours under shaking conditions (150 rpm). After enrichment, isolation was carried out from serially diluted samples (10^{-1}-10^{-6}). 0.1 ml of each dilution was plated on guaiacol agar plates (MSM + 1.5% agar + 0.2 mM guaiacol) and incubated for 48–72 hours. Colonies exhibiting reddish-brown halos around their growth on guaiacol-containing agar were considered presumptive laccase producers, as laccase oxidizes guaiacol to a polymer (Alshammary et al., 2025).

Secondary Screening and Quantitative Laccase Assay

Purified isolates were cultured in liquid MSM at pH 7 and 9, supplemented with 0.2 mM guaiacol, and incubated under identical conditions. After 120 hours, cultures were centrifuged at 10,000 × g for 10 minutes at 4°C, and the supernatant was used for enzyme assays. Laccase activity was determined at room temperature using guaiacol as a substrate. The reaction was performed in a 100 mM sodium acetate buffer (pH 5.0) containing 10 mM guaiacol. The reaction mixture consisted of 3.0 mL of buffer, 1.0 mL of guaiacol solution, and 1.0 mL of crude culture supernatant from the enzyme source, resulting in a final volume of 5.0 mL. The mixture was incubated for 10 minutes at room temperature in the dark and under static conditions, after which the absorbance was measured at 470 nm using a UV spectrophotometer (UV-1900, Shimadzu)(Vantamuri and Kaliwal, 2016).

One unit (U/mL) of laccase activity was defined as the amount of enzyme required to oxidize 1 µmol of guaiacol per minute under the assay conditions. Enzyme activity was calculated using the following equation:

$$\text{Enzyme Activity (U/mL)} = \frac{(Abs_{470} \times 4 \times V_t \times Dilution\ Factor)}{(\epsilon \times V_s)}$$

Where:

Vt = 5.0 mL → final volume of the reaction; Vs = 1.0 mL → enzyme sample volume; ε = 6740 $M^{-1}cm^{-1}$ → extinction coefficient of guaiacol.

Molecular identification of a potential isolate

The best laccase producer was characterized morphologically and biochemically, and further identification was carried out by 16s rDNA gene, for which the genomic DNA of the potential bacterial isolates was extracted, and the 16s rDNA gene was amplified using the universal primers (F, 5' AGAGTTTGATCCTGGCTCAG 3'; R, 5'TACGGYTACCTTGTTACTT 3')(Frank et al., 2008). Amplification was carried out in a thermal cycler (Applied Biosystems Veriti) using the following reaction profile: initial denaturation at 95°C for 3 min, followed by 35 cycles of denaturation at 95°C for 30 seconds, annealing at 55°C for 30 seconds, and extension at 72°C for 01 minute, with a final extension at 72°C for 5 min. The purified PCR product was sequenced, and the phylogenetic relationship of the isolate was determined by comparing the obtained sequence with sequences available in the GenBank database of the National Center for Biotechnology Information (NCBI) (Weisburg et al., 1991).

Media Optimization by One-Factor-at-a-Time (OFAT)

A One-Factor-at-a-Time (OFAT) approach was employed to optimize laccase production by systematically evaluating individual media components and culture conditions. Three basal media—Luria–Bertani, Nutrient Broth, and Minimal Medium—were compared, with Minimal Medium selected for its superior enzyme yield (Nandal et al., 2013). The best basal medium, which yielded good enzyme activity, was chosen for further analysis. The selected basal media supplemented with 1% w/v carbon sources (fructose, galactose, maltose, lactose, xylose, sucrose, dextrose, starch, glycerol, tri-sodium citrate, sodium acetate, cellulose). Different organic and inorganic nitrogen sources at a concentration of 0.2% w/v (yeast extract, ammonium sulfate, sodium nitrate, urea, peptone, beef extract, casein, gelatin) were tested to identify the most supportive substrates for laccase induction. Among these, the best carbon and nitrogen sources were tested at different concentrations of 0.25, 0.50, 1.00, 2.00, 4.00, and 8.00% w/v, and 0.05, 0.10, 0.20, 0.40, 0.80, and 1.60% w/v, respectively(Arumugam and Uthandi, 2024; El-Bendary et al., 2021). Nine metal ions ($CuSO_4$, $FeCl_3$, KCl, $ZnCl_2$, $MgCl_2$, $MnCl_2$, $NiCl_2$, NaCl, $CaCl_2$) were tested at 0.01 mM and 0.1 mM concentrations to assess the role of trace elements. Furthermore, the influence of pH was studied using five buffer systems with a concentration of 10 mM: Tris–HCl (pH 7.0, 8.0, 9.0, 10.0), phosphate (pH 7.0), carbonate–bicarbonate (pH 9.0 and 10.0), Tris-citrate (pH 8.0), and sodium acetate (pH 7.0). The tolerance and enzyme activity production of the strain under the effect of surfactants at concentrations of 0.1mM, 1 mM, and 5mM (Tween 80, SDS), inhibitor (EDTA), and organic solvents at concentrations of 5% and 20% (acetone, ethanol, methanol) were checked (Britos et al., 2018).

Media Optimisation by Plackett–Burman Design (PBD)

The Plackett-Burman (PB) design is a powerful technique for screening and evaluating variables that affect enzyme production (Plackett and Burman, 1946). In the present study, seven factors, including cellulose, sucrose, urea, beef extract, peptone, and $MnCl_2$ and $MgSO_4$, were screened using a PB design to identify the significant factors affecting laccase enzyme production (Table 1). The experimental design for screening variables is presented in Table 2. All variables were treated as numerical factors and explored at two widely spaced levels: low and high. The following equation calculated the individual parameters of laccase production:

$$E(Xi) = 2(\Sigma M - \Sigma M)/N$$

Where E is the effect of the parameter under study on Laccase production at which the parameter was at its highest and lowest, respectively, and N is the total number of trials.

An experimental error was estimated by calculating the variation among the dummy variables as

$$Veff = (Ed)/n$$

Where *V*eff is the variance of the effect of level, Ed is the dummy variable effect, and n is the number of dummy variables used. The standard error (SE, Es) of the concentration effect was the square root of the variance of an impact, and the significance level(P-value) of each concentration effect was determined using Student's t-test.

$$t(Xi) = E(Xi)/Es$$

Where E (Xi) is the effect of variable Xi.

A 12-run experimental matrix was generated using Design-Expert software, with randomized combinations of high and low levels for each factor. Each run was conducted in 100 mL Erlenmeyer flasks containing 50 mL of LB medium supplemented with 0.02% guaiacol and 0.2 mM $CuSO_4$. Cultures were incubated at 35 ± 2°C for 72 hours under steady-state conditions.

Table 1
Components and their values used in Plackett-Burman design for laccase production using *Proteus mirabilis* JB1

1	Component	Low Value	High Value
	Cellulose	**0.1%**	**1.2 g%**
2	Sucrose	0.1%	1.5g%
3	Urea	0.05g%	2 g%
4	Beef Extract	0.05 g%	2 g%
5	Peptone	0.05 g%	2 g%
6	MnCl2	0.01mM	0.1 mM
7	MgSO4	0.01mM	0.1mM

Table 2
Plackett–Burman design generated by the fractional rotation of a full factorial design, where X1–X7 are independent variables and D1–D2-D3-D4 are dummy variables.

Run No		X1	X2	X3	X4	X5	X6	X7	X8	X9	X10	X11
	Laccase Activity (U/ml)	Cellulose	Sucrose	Urea	Beef Extract	Peptone	MnCl2	MgSO4	D1	D2	D3	D4
1	1	High	High	low	High	High	High	low	low	low	High	low
2	1.27	low	High	High	low	High	High	High	low	low	low	High
3	**1.89**	**High**	**low**	**High**	**High**	**low**	**High**	**High**	**High**	**low**	**low**	**low**
4	0.9	low	High	low	High	High	low	High	High	High	low	low
5	1.22	low	low	High	low	High	High	low	High	High	High	low
6	1.32	low	low	low	High	low	High	High	low	High	High	High
7	1.2	High	low	low	low	High	low	High	High	low	High	High
8	1	High	High	low	low	low	High	low	High	High	low	High
9	1.65	High	High	High	low	low	low	High	low	High	High	low
10	1	low	High	High	High	low	low	low	High	low	High	High
11	1.3	High	low	High	High	High	low	low	low	High	low	High
12	1.6	low	low	low	low	low	low	low	low	low	low	low

Media Optimization by Central Composite Design (CCD)

A Central Composite Design (CCD) was employed under Response Surface Methodology (RSM) to fine-tune the concentrations of key media components identified through Plackett-Burman Design. CCD enables modeling nonlinear relationships and interactions among variables, allowing the prediction of optimal conditions for maximum laccase production (Othman et al., 2021). Based on statistical significance and biological relevance, three variables were selected for CCD: i.e., A: Urea; B: Cellulose; C: Magnesium sulfate ($MgSO_4$). Each variable was studied at five coded levels: −α, − 1, 0, + 1, and + α, where α = 1.68 for rotatability. The actual concentrations corresponding to these levels are shown in Table S1.

A total of **20 experimental runs** were generated using Design-Expert software, and were conducted in 250 mL Erlenmeyer flasks containing 100 mL of Luria–Bertani (LB) medium supplemented with 0.02% guaiacol and 0.2 mM $CuSO_4$. Cultures were incubated at 35 ± 2°C for 72 hours under steady-state conditions.

Model adequacy was evaluated using ANOVA, R^2, adjusted R^2, predicted R^2, and lack-of-fit tests. Response surface plots and contour diagrams were generated to visualize the effects and interactions among variables.

Software and data analysis

The experimental design data were statistically analyzed and interpreted using Design-Expert software version 8.0 (Stat-Ease Inc., Minneapolis, MN, USA).

Biological Synthesis of Selenium Nanoparticles and Laccase Coating

Selenium nanoparticles (SeNPs) were biologically synthesized using the cell-free supernatant of the optimized laccase-producing microbial strain to enhance laccase's catalytic stability and reusability for environmental applications. Subsequently, laccase was immobilized onto the surface of SeNPs to form a nanobiocatalyst system (Lac@SeNPs), which was characterized using multiple analytical techniques.

Immobilization of Laccase onto SeNPs (Lac@SeNPs)

Partial Purification of Laccase

The microbial strain was cultivated under optimized conditions in LB medium supplemented with 0.02% guaiacol and 0.2 mM $CuSO_4$ to induce laccase production. After 72 hours of incubation at 35 ± 2°C and under steady-state conditions, the culture was centrifuged at 10,000 × g for 10 minutes at 4°C. The resulting cell-free supernatant was filtered through a 0.22 µm membrane to ensure sterility (Kasirajan et al., 2021).

Laccase from the clarified supernatant was precipitated with ammonium sulfate to 80% saturation. The protein precipitate was dissolved in 50 mM Tris buffer (pH 8.0) and dialyzed against the same buffer at 4°C overnight to remove residual ammonium sulfate (Illuri et al., 2021).

Synthesis and Immobilization of Selenium Nanoparticles

Selenium nanoparticles (SeNPs) were produced using partially purified bacterial laccase as the biocatalyst. In particular, 5 ml of the enzyme solution was stirred with 30 ml of 10 mM sodium selenite. The reaction was incubated at 37ºC for 48 hours, and nanoparticle formation was observed by a noticeable color change from colorless to brick red (Abdulmumini et al., 2025).

Characterization of Lac@SeNPs by UV–Visible Spectroscopy

UV–Visible spectroscopy differentiated biologically synthesized selenium nanoparticles (SeNPs) and laccase-coated selenium nanoparticles (Lac@SeNPs). Spectral measurements were conducted on a double-beam UV–Vis. spectrophotometer (Shimadzu UV-1900) over 200–800 nm. SeNPs exhibited an inherent absorbance peak in the 250–300 nm region, confirming nanoparticle formation via surface plasmon resonance. Conversely, a minor shift and broadening of the peak occurred, along with the development of extra shoulders at 280–320 nm, which is characteristic of effective enzyme conjugation and protein–nanoparticle interaction. This spectral change facilitated the creation of a robust nanobiocatalyst system viable for further use in cypermethrin degradation (Ullah et al., 2021).

Characterization of laccase-coated selenium nanoparticles (Lac@SeNPs)

Fourier Transform Infrared (FTIR) spectroscopy was used to identify the functional groups responsible for stabilising biologically synthesised selenium nanoparticles (SeNPs) and to validate successful immobilisation of laccase onto their surface. Air-dried laccase-coated SeNPs (Lac@SeNPs) were powdered and blended with spectroscopic-grade potassium bromide (KBr) at 1:100 to form translucent pellets. Spectral analysis was conducted in the range of 4000–400 cm^{-1} at a resolution of 4 cm^{-1}. FTIR measurements were subcontracted to the Center of Excellence in Vapi, which has a high-resolution PerkinElmer Fourier Transform Infrared (FTIR) spectrometer for spectral acquisition (Zhao et al., 2025). Particle size distribution and zeta potential of laccase-coated selenium nanoparticles were measured using the NanoPlus Particle Size and Zeta Potential Analyzer (Particulate Systems, India). DLS determined the hydrodynamic diameter and PDI at 25°C. Zeta potential was calculated using Electrophoretic Light Scattering and the Smoluchowski equation (Oliveira et al., 2026).

Cypermethrin Degradation Assay

Cypermethrin degradation was assessed using three distinct biocatalytic treatments: (i) direct application of the laccase-producing microbial strain, (ii) partially purified laccase enzyme, and (iii) laccase-coated selenium nanoparticles (Lac@SeNPs). The assay was conducted in Minimal Salt Medium (MSM) supplemented with cypermethrin at concentrations ranging from 0.3 mM to 1.0 mM. For the microbial treatment, actively growing cultures were inoculated into MSM containing cypermethrin and incubated at 35 ± 2°C under steady-state conditions. In parallel, purified laccase (10 U/mL) and Lac@SeNPs (equivalent enzyme loading) were added to separate reaction sets under identical conditions. Samples were withdrawn at defined time intervals (0, 12, 24, 48, and 72 hours), and residual cypermethrin was extracted using ethyl acetate. The degradation of cypermethrin was preliminarily evaluated by monitoring changes in its characteristic absorption profile using a UV-Visible spectrophotometer over the wavelength range 200–400 nm. Alterations in the absorption characteristics (λmax) of cypermethrin were observed and

analyzed by comparing them with the control sample to determine the degree of pesticide degradation. A reduction or complete disappearance of absorbance at λmax indicated that cypermethrin was degraded using the proposed nanobiocatalytic technique (Kansal et al., 2023). Quantification was performed via FTIR and gas chromatography (GC). For GC, an electron capture detector (ECD) equipped GC with an HP-5 capillary column under programmed temperature (initial 150°C ramped to 260°C) in a carrier gas of nitrogen flowing at 1 mL/min; identification and quantification by retention times and peak areas against authentic standards, with method validation involving determination of recovery rates, detection and quantification limits to allow accurate and precise analysis of cypermethrin degradation. (He et al., 2022)

Results

Primary screening and isolation of microbial strain

A total of 21 morphologically distinct microbial isolates were obtained from five different environmental samples; among these isolates, 03 were from industrial effluent, 01 from industrial biological sludge, 05 from industrial chemical sludge, 10 from agro waste composting soil, and 02 from contaminated soil from an industrial area. All these isolates were subjected to primary screening on guaiacol-supplemented agar plates. Among these, 12 isolates exhibited reddish-brown zones indicative of extracellular laccase activity. All 12 isolates underwent secondary screening to quantify laccase production, followed by screening for potential laccase producers.

Secondary screening and Quantitative Laccase activity to select potential isolate

A total of 12 morphologically distinct bacterial isolates were cultivated in liquid production medium, and extracellular laccase activity was quantified using guaiacol as the chromogenic substrate. Among these, isolate JB1 exhibited the highest laccase activity, i.e., 0.249 U/mL and 0.156 U/mL at pH 9 and pH 7, respectively, after 96 hours of incubation at 35 ± 2°C under steady state conditions. Enzymatic activity was determined by monitoring guaiacol oxidation, and results were expressed as units per millilitre (U/mL) of culture supernatant. The activity range across all isolates varied from 0.001 to 0.220 U/mL at pH 9 and 0.007 to 0.156 U/mL at pH 7, as shown in Table S2.

Molecular identification of a potential isolate

The potential isolate JB1 was molecularly identified by 16S rDNA sequencing and compared with the NCBI database using BLASTn, showing 99% similarity to a strain with accession number OP860660. The phylogenetic tree was prepared using the neighbour-joining method (Figure S1). Based on morphological, biochemical, and molecular identification, the isolated strain was classified as *Proteus mirabilis*, and the sequence has been deposited in NCBI GenBank under accession number PQ160485.

Optimisation of Laccase Production Using the OFAT Approach

Among the three basal media used for cultivation, laccase activity was highest in LB (0.240 U/mL). Testing several carbon sources at 1% (w/v), cellulose supported the highest laccase activity (0.638 U/mL), followed by sucrose (0.558 U/mL), lactose (0.467 U/mL), and xylose (0.355 U/mL). The comparative data have been summarized in Fig. 1 (a). Further optimization of cellulose revealed that only 0.25% (w/v) was required to enhance laccase production (0.705 U/ml), Fig. 2 (a). Among the tested nitrogen sources (0.2% w/v), organic sources, especially urea (0.792 U/mL) and beef extract (0.789 U/mL), were found to improve laccase production compared with inorganic sources such as ammonium sulfate and sodium nitrate (Fig. 1(b)). Concentration optimization revealed that the optimal nitrogen concentration was 0.8% w/v, resulting in an enhanced laccase activity of 0.798 U/mL (Fig. 2(b)). The influence of **pH** on laccase biosynthesis, shown in Fig. 1(c), indicated the highest enzyme activity at pH 9.0 in a 10 mM Tris–HCl buffer, demonstrating that the bacterial strain can tolerate alkaline conditions, thereby improving enzyme production and secretion. Moreover, the enzyme proved highly stable at alkaline pH. Metal ion screening indicated that $MnCl_2$ (0.999 U/mL), $MgSO_4$ (0.981 U/mL), $CaCl_2$(0.900 U/mL), NaCl (0.905 U/mL) and KCl (0.875 U/mL) ions had the highest activity observed at 0.1 mM, whereas $CuSO_4$ (0.952 U/mL), $FeSO_4$ (0.958 U/mL) and $NiCl_2$ (0.915 U/mL) influenced laccase activity at 0.01 mM (Fig. 1(d)).

The effects of surfactants, inhibitors, and organic solvents were studied to assess enzyme stability under industrially relevant conditions. For comparison, the untreated enzyme is used as the 100% activity standard. SDS was found to significantly inhibit the enzyme's activity, resulting in ~ 53–70% of the activity at all concentrations. On the other hand, the non-ionic surfactant, Tween 80, showed relatively little inhibition, with residual activity of 64–74%. The enzyme showed moderate activity (~ 44–67%) in the presence of EDTA. The enzyme activity remained relatively high in methanol and ethanol at 5% concentration, with residual activity of 81 and 65%, respectively. However, inhibition of the enzyme by acetone resulted in 20% residual activity at a concentration of 20% (v/v). (Figure S2)

Media Optimisation by Plackett–Burman Design (PBD)

A Plackett–Burman Design (PBD) was employed to statistically evaluate the influence of 07 independent variables on laccase production. Where glucose and sucrose were found to be the best carbon sources, while urea, beef extract and peptone were chosen as the most suitable nitrogen sources. Moreover, $MnCl_2$ and $MgSO_4$ were the metal ions that most strongly stimulated enzyme synthesis. CuSO4 was added to each flask at a concentration of 0.01 mM by default, along with other factors. These factors exerted a considerable impact on laccase biosynthesis by the isolated strain and were thus considered for optimisation using a Plackett-Burman Design (PBD). In the current research, however, other nitrogen sources and metal ions were found to be more effective, suggesting that the JB1 strain possesses unique characteristics. The Plackett-Burman method was used to examine the significance of seven factors, comprising various carbon and nitrogen sources and metal ions, in a 12-experiment design at two concentration levels. Experiments were performed in statically operated submerged fermentation at pH 9 and 37°C for 3 days. High and low concentrations for each factor are listed in Table 1. Experimental data and their corresponding effects, standard errors, t-ratios, p-values, and confidence levels are shown in Tables 2 and 4.

According to the statistical analysis, cellulose, urea, and $MgSO_4$ played significant roles in laccase synthesis, with each having a confidence level above 98%, making them the most important parameters to optimise.

CCD-RSM

A CCD has been adopted to explore interactions among the important factors identified by the Plackett-Burman Design and to determine their optimal values for improved laccase production. A total of 20 experiments were carried out to come up with a quadratic model having three independent variables, namely cellulose (A), urea (B), and $MgSO_4$ (C), at varying concentrations. The experimental design, along with corresponding predictions and observations, is shown in Table 3.

Table 3
The experimental CCD with actual and coded levels of variables and the response function

Std		Factor 1		Factor 2		Factor 3		Response 1	
	Run	A: Cellulose		B: Urea		C: MgSO4		Observed	Predicted
		gm %	Coded	gm %	Coded	mM	Coded	U/ml	U/ml
1	19	0.5	-1	0.7	-1	0.05	-1	1.94	1.94
2	17	1.5	1	0.7	-1	0.05	-1	2.23	2.23
3	14	0.5	-1	2.5	1	0.05	-1	1.94	1.81
4	16	1.5	1	2.5	1	0.05	-1	2.08	2.08
5	15	0.5	-1	0.7	-1	0.15	1	1.97	1.97
6	12	1.5	1	0.7	-1	0.15	1	2.03	2.03
7	18	0.5	-1	2.5	1	0.15	1	1.71	1.71
8	5	1.5	1	2.5	1	0.15	1	1.97	1.97
9	9	0.159104	-α	1.6	0	0.1	0	2.03	2.03
10	8	1.8409	+α	1.6	0	0.1	0	2.3	2.3
11	11	1	0	0.086387	-α	0.1	0	2.08	2.08
12	13	1	0	3.11361	+α	0.1	0	1.64	1.64
13	10	1	0	1.6	0	0.01591	-α	1.73	1.85
14	7	1	0	1.6	0	0.18409	+α	1.86	1.86
15	1	1	0	1.6	0	0.1	0	1.87	1.87
16	3	1	0	1.6	0	0.1	0	1.86	1.86
17	6	1	0	1.6	0	0.1	0	1.88	1.88
18	4	1	0	1.6	0	0.1	0	1.88	1.88
19	2	1	0	1.6	0	0.1	0	1.87	1.87
20	20	1	0	1.6	0	0.1	0	1.87	1.7

Table 4
Statistical analysis of components for laccase production by *Proteus mirabilis* JB1

Components	Effect	t value	p Value	% Significance
Cellulose	0.2966667	4.94	0.007817	99.21832
Sucrose	-0.11	1.83	0.141228	85.87724
Urea	0.41	6.83	0.002403	99.75966
Beef E	0.0866667	1.44	0.223287	77.67128
Peptone	-0.0866667	1.44	0.223287	77.67128
MnCl2	0.1833333	3.06	0.037658	96.23415
MgSO4	0.3766667	6.28	0.003283	99.67172

The production of the laccase enzyme can best be modeled using the following model:

$Y = 1.85 + (0.0977*A) - (0.0981*B) - (0.0488*C) + (0.0225*A*B) - (0.03*A*C) - (0.005*B*C) + (0.1087*A^2) + (0.0009*B^2) + (0.0097*C^2)$

in which Y = production of the laccase enzyme (U/ml), A = Cellulose (g%), B = Urea (g%), and C = $MgSO_4$(mM)

The model F-value of 21.13 indicates statistical significance, as the probability of obtaining that value by chance alone is only 0.01%. The p-values for the terms A, B, C, and A^2, all less than 0.05, indicate significance for the model factors, suggesting that linear and quadratic cellulose are vital to enzyme production. The F value for the lack-of-fit term (3.58) was not significant ($p > 0.05$), indicating that the model fits the experimental data well, as represented in Table 5. In addition, the model fits the experimental data well, with a high coefficient of determination (R^2) and a low CV.

Table 5
Analysis of variance for the fitted quadratic polynomial model for level optimization of laccase production using *Proteus mirabilis* JB1

Source	Sum of Squares	df	Mean Square	F-value	p-value	
Model	0.4775	9	0.0531	21.13	< 0.0001	significant
A-Cellulose	0.1303	1	0.1303	51.89	< 0.0001	significant
B-Urea	0.1315	1	0.1315	52.35	< 0.0001	significant
C-MgSO4	0.0325	1	0.0325	12.93	< 0.0049	significant
AB	0.004	1	0.004	1.61	0.2329	
AC	0.0072	1	0.0072	2.87	0.1213	
BC	0.0002	1	0.0002	0.0796	0.7835	
A^2	0.1704	1	0.1704	67.85	< 0.0001	significant
B^2	0	1	0	0.0047	0.9468	
C^2	0.0014	1	0.0014	0.5447	0.4775	
Residual	0.0251	10	0.0025			
Lack of Fit	0.0196	5	0.0039	3.58	0.0939	not significant
Pure Error	0.0055	5	0.0011			
Cor Total	0.5027	19				

Response surface plots and contour graphs were generated to examine parameter interactions and identify optimal points. The interaction between cellulose and urea (Fig. 3) showed that high cellulose concentrations increased laccase production, whereas high urea concentrations inhibited it. The interaction between cellulose and $MgSO_4$ indicated that higher concentrations of cellulose coupled with lower concentrations of $MgSO_4$ increased enzyme production, while high $MgSO_4$ concentrations decreased enzyme production. This is due to interference from high concentrations of inorganic ions, which can cause an osmotic imbalance. As shown in Fig. 4, maximum laccase activity was achieved at higher cellulose concentrations with reduced $MgSO_4$ levels. In contrast, elevated $MgSO_4$ combined with high cellulose suppressed enzyme yield, indicating the need for balanced nutrient–ion conditions for optimal biosynthesis. The interaction between urea and $MgSO_4$ (Fig. 5) also showed that low concentrations of the two variables favored laccase production.

This study makes it clear that laccase production requires a more complex interaction between nutrients and the environment. Synergistic effects observed with high cellulose and low nitrogen concentrations suggest a shift toward secondary metabolism for enzyme production. Antagonistic effects observed with higher salt concentrations may indicate that the cell is under stress.

Validation of the quadratic model

To verify the optimized medium and culture conditions, laccase production was performed twice under the specified conditions. The average laccase production was 2.300 U/mL, higher than the predicted 2.218 U/mL. The high correlation between experimentally observed and model-predicted values demonstrates that the model reliably predicts laccase production in *Proteus mirabilis* JB1.

Characterization of Lac@SeNPs

A distinct visual transformation in the reaction mixture provided preliminary evidence of laccase-mediated biosynthesis of selenium nanoparticles (SeNPs). The initially colorless sodium selenite solution developed a characteristic ruby-red color after 24 h of incubation (Figure S3), a well-established indicator of SeNP formation. UV further substantiated the formation of SeNPs–Visible spectroscopic analysis, which revealed a pronounced absorption peak at 300–374 nm (Figure S4). This absorption maximum (λ_max) falls within the previously reported range for biologically synthesized SeNPs (240–560 nm), thereby validating the successful formation of nanoparticles in the present system (Ahamad Tarmizi et al., 2023).

To elucidate the molecular interactions underlying nanoparticle synthesis and stabilization, Fourier-transform infrared (FTIR) spectroscopy was employed to compare the spectra of native laccase and the synthesized Lac@SeNPs (Figure S5). The FTIR spectrum of laccase exhibited prominent bands at 430, 451, 1037, 1642, 2103, and 3368 cm^{-1}. The peaks at 430 and 451 cm^{-1} correspond to Cu-O/Cu-N vibrations, indicative of metal-ligand interaction and confirming the multicopper nature of the laccase enzyme. The glycosidic linkage observed at 1037.45, which corresponds to C-O/C-N stretching, confirms the glycoprotein nature of the enzyme. The amide I band at 1642.03 cm^{-1} corresponds to C = O stretching of peptide bonds and reflects the secondary structural elements of proteins, including α-helices and β-sheets. The broad band at 3368.06 cm^{-1} is attributed to O–H and N–H stretching vibrations, suggesting extensive hydrogen bonding. Minor peaks in the range of 2103 cm^{-1} may be assigned to C ≡ C stretching or interactions involving metal-associated organic moieties.

Subsequent laccase-coated nanoparticle formation, significant spectral modifications were observed in the FTIR profile of Lac@SeNPs. Characteristic peaks were detected at 444.49, 1638.83, 2105.38, and 3439.94 cm^{-1}. The metal-shift O (444.49 Cm-1) vibration indicates a strong interaction between selenium and a proteinaceous environment. The persistence of the amide I band at 1638.83 cm^{-1} indicates the continued association of proteinaceous components with the nanoparticle surface, highlighting their role in capping and stabilizing the nanoparticle. The disappearance of the C–O stretching band at 1037.45 cm^{-1} suggests the involvement of glycosidic moieties in the reduction process, possibly through structural modification or cleavage. The emergence of a distinct peak at 2105.38 cm^{-1} indicates the formation of selenium–organic interactions, likely due to selenium binding to functional groups within the enzyme matrix. Furthermore, the slight shift in the broad O–H/N–H stretching band reflects changes in hydrogen-bonding patterns, indicative of conformational rearrangements during nanoparticle synthesis. The DLS results of the synthesized laccase-coated selenium nanoparticles (Lac-SeNPs) showed a single distinct peak corresponding to an average hydrodynamic diameter of 376.7 nm with a polydispersity index (PDI) of 0.206. The lower PDI value indicates a narrower size distribution, thereby indicating the formation of a homogeneous dispersion of nanoparticles. Also, the measured zeta potential of − 20.73 mV suggests moderate stability of the colloid. (Figure S6).

Cypermethrin degradation assay

Identification of cypermethrin was initially performed using UV-Visible spectroscopy. The compound exhibited an absorption maximum (λmax) at approximately 268 nm, attributable to aromatic conjugation. In the course of degradation of this compound, there was a decrease in absorbance at λmax in all concentrations ranging from 0.3 mM to 1.0 mM, as presented in Figures S7 & S8.

Among these samples, the 1 mM sample was analyzed by FTIR to assess structural modifications of cypermethrin upon interaction with various biocatalytic systems, as shown in Table S3a. The untreated control sample (C; cypermethrin) displayed typical absorption peaks for ~ 3369 cm^{-1} (O–H/N–H), 2091 cm^{-1} (C ≡ X stretching), 1640 cm^{-1} (C = C/C = O), and halogen peaks at 413–746 cm^{-1}, confirming its aromatic and halogenated structure. During treatment, the samples exhibited gradual

spectral changes, indicating stepwise degradation of the pesticide. The B sample (B: Direct inoculation of *Proteus mirabilis* JB1 strain) showed the absence of prominent aromatic ring peaks with minimal shifts in halogen peaks, denoting the breakdown of aromatic rings and partial conversion. In the case of E (E: Partially purified laccase enzyme), the presence of broadened peaks in the halogen region, alongside retention of the C = C band, indicates moderate degradation with partial structural preservation.

However, the most drastic change in peak intensity was observed in the Se + BE (Se + BE: Lac@SeNPs) sample, wherein the peak for C ≡ X was absent, along with broadened peaks in the metal interaction. These findings suggest that enzyme-coated nanoparticles are the best option for such applications, as they provide greater stability and sustainability for the enzyme (Figure S9).

Confirmation of cypermethrin degradation by GC–MS and its metabolites profiling:

Further confirmation of cypermethrin degradation was obtained by GC–MS analysis (Table S3b). In the control test, the cypermethrin peak was detected at 25.0-25.3 min, with an area of 3,521,090, corresponding to 100% residual pesticide. On the contrary, no cypermethrin peak was detected in any of the treated tests with B, E, and Se + BE, indicating complete degradation, with 100% efficiency. This finding provides robust corroboration with FTIR and shows complete degradation of cypermethrin. Metabolites obtained from GC-MS analysis include: Long chain hydrocarbons (heneicosane, eicosane, tetratriacontane), Oxygenated intermediates (ethyl acetate derivatives), Phenols (2,4-di-tert-butylphenol), Alkane derivatives. From this observation, it can be concluded that cypermethrin degradation is associated with oxidation of ester linkages, aromatic ring fragmentation, and further conversion to simpler aliphatic/phenolic intermediates. The GC chromatogram is shown in Figure S10. It is important to note that the Se + BE treatment system yielded balanced intermediates, suggesting an efficient degradation pathway.

Discussion

Industrial effluents and effluent-contaminated soil are ideal niches for extremophilic microorganisms due to their harsh physicochemical conditions; such environments are promising sources for bioprospecting novel extremozyme-producing microorganisms. Microbial strains adapted to such chemical stress are physiologically capable of producing pollutant-degrading enzymes such as laccases (Chandel et al., 2026). Primary screening includes plate assays to quickly assess the ability of isolates to secrete laccase enzymes identified from reddish-brown colorations surrounding the colonies on guaiacol, a model substrate for lignin degrading enzymes such as laccases and peroxidases (Mehandia et al., 2020), while secondary screening involves submerged fermentation and spectrophotometric assays to measure enzyme production, activity, and stability in greater detail (Wiśniewska et al., 2021). This systematic approach selects the most promising candidates for further optimization. Variation in laccase activity among isolated strains reveals the metabolic diversity inherent in bacterial communities from diverse environmental sources. Previous reports highlight the suitability of rapid screening to identify potential isolates for further research (Kumar et al., 2025).

Initial screening of media components was conducted using the One-Factor-at-a-Time (OFAT) method to identify key parameters influencing laccase production (Deepa et al., 2020). Optimizing laccase synthesis via the OFAT technique revealed that laccase production was significantly affected by both nutritional and physicochemical factors. One important factor is the availability of organic nitrogen sources, which are essential for enzyme production and provide amino acids, vitamins, and growth factors. Therefore, an environment rich in nitrogen sources is more likely to induce enzyme synthesis than other media, such as Minimal salt medium and Nutrient broth. The previous report also supports recent findings indicating the major role of nitrogen in enhancing laccase production (Colla et al., 2023). The present study stated the importance of complex carbon sources, such as cellulose, which increased laccase production compared with simple sugars, which were usually better inducers. It suggests that, in the presence of an inducer such as guaiacol, complex carbon sources can more effectively promote growth and enzyme formation than readily degradable carbon sources (Mahuri et al., 2023). The increased enzyme activity in the presence of guaiacol on complex carbon sources can be explained by the substrate's dual nature: it serves not only as a nutrient but also as an inducer. The rapid utilization of simple sugars, such as glucose and sucrose, enables faster microorganism growth while suppressing secondary metabolism through catabolic repression. Guaiacol, a representative

aromatic molecule, serves as a diagnostic substrate that induces laccase formation by stabilizing the enzyme's copper-binding active site. The mechanisms of gene induction described above align with the ecological roles of fungi and bacteria as lignocellulose degraders, in which aromatic compounds function as inducers of enzymatic reactions (Shraddha et al., 2011). For the nitrogen source, the observation aligns with previous reports showing that complex organic nutrients stimulate the biosynthesis of secondary metabolites and enzymes in fungi and bacteria (Parshad et al., 2025; Sun et al., 2024). Excess nitrogen appeared to repress enzyme synthesis, possibly via catabolite repression mechanisms, in which high nutrient availability diverts metabolic flux toward primary metabolism rather than secondary enzyme production (Cunningham et al., 2000). Unlike most reported laccases, which typically show high activity at acidic to neutral pH and low stability at alkaline pH (Benavides et al., 2024), JB1 exhibits stability of laccase activity at an alkaline pH of 11, distinguishing it from the majority of reported laccase-producing strains. Such extremozymes have substantial direct applications in all the remedial and biotechnological applications performed under alkaline conditions. Metal ions play a major role in laccase function, as previously reported. Also, previous reports supported the present findings of the influence of copper, manganese, and magnesium ions on laccase activity (Benavides et al., 2024; Stajic et al., 2006). Surfactants can affect enzyme activity in different ways. Ionic surfactants typically reduce enzyme activity, likely by disrupting hydrophobic interactions and destabilizing protein folding. On the other hand, non-ionic surfactants often have little effect on activity, and sometimes even help dissolve substrates without harming the enzyme’s structure (Liu et al., 2025). Inhibitors such as metal chelators often lower enzyme activity by sequestering essential metal ions, thereby impairing catalytic efficiency. In laccases, these inhibition patterns show that the enzyme depends on metal cofactors, especially copper (Cu), which is needed for its catalytic function (Elsayed et al., 2023). Organic solvents affect enzymes differently depending on their concentration. At low amounts, they can help substrates dissolve and make enzymes more accessible. At higher levels, they can stop enzyme activity by causing proteins to lose their structure and damaging membranes. Some microbes can tolerate polar solvents, which suggests their enzymes are either more stable or supported by cofactors (Jafari et al., 2020).

PBD and CCD analyses from earlier investigations have shown that glucose, yeast extract, and metal ions such as copper and iron significantly stimulate laccase formation in *Enterobacter* species (Hosseini et al., 2025). It is well known that certain inorganic compounds play important roles in laccase production and secretion. Notably, NH_4Cl, $MnSO_4$, and $CuSO_4$ have a stimulatory effect on laccase production (Abdelgalil et al., 2022). The present study identifies cellulose, urea, and $MgSO_4$ as potential media components. These results corroborate earlier studies showing that, in addition to serving as a substrate, more complex carbon sources, such as cellulose, act as inducers, stimulating laccase synthesis via ligninolytic pathways (Elisashvili et al., 2008; Piscitelli et al., 2011). In other words, the increase in enzyme yield at higher cellulose concentrations could be linked to upregulation of laccase-encoding genes, induced by oxidative enzymes that degrade recalcitrant polymers (Janusz et al., 2020). Induction, in turn, is usually mediated by transcriptional regulators responding to lignocellulosic substrates (Mate and Alcalde, 2015). On the contrary, increased nitrogen concentration appears to reduce the efficiency of laccase synthesis, most likely via nitrogen catabolic repression (NCR), a regulatory pathway used by many microorganisms to repress secondary metabolism, particularly ligninolytic enzymes, when nitrogen is abundant (Baldrian, 2006). In line with the theory described above, the decreased enzyme yield efficiency observed as urea concentration increases can be explained within the NCR framework. Moreover, the effects of $MgSO_4$ provide insights into the role of mineral ions in regulating enzyme production. Although metal ions are important for the structural stability and function of cells and enzymes, their levels should be carefully controlled. While an appropriate amount of magnesium ions (Mg^{2+}) can enhance enzyme stability and metabolism, higher concentrations can disrupt the balance among ionic concentration, osmotic pressure, and protein folding or secretion. This phenomenon has been previously observed, with metal ions activating or inhibiting reactions depending on concentration and the cellular systems involved (Najafabadipour et al., 2021).

Despite the growing interest in enzyme-assisted nanoparticle synthesis, the application of laccase for this purpose remains largely unexplored. In this context, the present study provides novel evidence for the utilization of laccase in the green synthesis of SeNPs. Enzymes facilitate the reduction of metal ions by donating electrons, thereby forming zero-valent nanoparticles. Additionally, biomolecular functional groups stabilize nanoparticles through electrostatic interactions and surface binding (Pasinszki and Krebsz, 2020). The diameters have been similar to those previously recorded for other biogenic or protein-coated selenium nanoparticles (Zhang et al., 2024). Despite the size of the synthesized particles being higher than that of the

bare selenium nanoparticles (50–200 nm) (Geng et al., 2025), this is a usual trend that has been observed when an enzyme or protein is used for coating, owing to surface adsorption of proteins, hydration layer formation, and interaction between the coated particles. The zeta potential value is attributed to the ionizable groups (amino acids) of the adsorbed laccase molecule at the nanoparticle surface. According to previous reports, the zeta potential values for selenium nanoparticles capped with proteins range between − 15 and − 35 mV (Tugarova et al., 2018). This implies that the resulting nanoparticles exhibit good dispersion stability and successful enzyme functionalization. The results provide sufficient evidence that stable laccase-coated selenium nanoparticles were formed and that laccase is an effective stabilizing and capping agent for their synthesis. SeNP provides a greater surface area for enzyme immobilization, reduces enzyme denaturation, and increases the biocatalyst's thermal and pH stability and reusability. Thus, the Lac-SeNP system is a sustainable alternative for remediating highly contaminated environments. Previous studies have shown that no strains have the potential to degrade 100% of cypermethrin within a short period of time (72 hours) (Bhatt et al., 2020; Das et al., 2022; Huang et al., 2018).

Conclusion

A recent study introduces a novel technique for decontaminating cypermethrin using a nanobiocatalyst containing extremophilic enzymes. The laccase-producing bacterial strain *Proteus mirabilis* JB1 demonstrated stability across diverse environments and was thus identified as a promising source of robust enzymes for future applications.

Enzyme production in the selected microorganism was improved through systematic optimization. Initial screenings in minimal salt and Luria-Bertani media yielded enzyme activities of 0.220 U/mL and 0.240 U/mL, respectively. Using the one-factor-at-a-time method, cellulose at 0.25% was identified as the optimal carbon source (0.705 U/mL), and urea at 0.8% as the optimal nitrogen source (0.798 U/mL). At pH 9, the addition of $MnCl_2$ further increased activity to 0.999 U/mL. The Plackett-Burman Design identified cellulose (1.5% w/v), urea (0.7% w/v), and $MgSO_4$ (0.05 mM) as the most significant factors for enzyme production. Central Composite Design was then used to evaluate their interactions, raising enzyme activity to 2.300 U/mL. This process resulted in a 9.58-fold increase from the initial value. Combining traditional and statistical optimization methods significantly enhanced enzyme production. These results demonstrate strong potential for practical applications.

Laccase-coated selenium nanoparticles showed superior catalytic activity and stability, achieving complete cypermethrin degradation within 72 hours, as confirmed by GC-MS analysis. This method provided more efficient pesticide decontamination than conventional approaches and did not produce intermediate products.

In summary, this study bridges enzyme engineering and nanobiotechnology, offering an advanced solution for efficient, sustainable pesticide degradation.

Declarations

Authors Contribution

Conceptualization and Supervision; N.P., Methodology; J.B., and V.P., Formal analysis; N.P., writing—original draft; J.B., and V.P., Review and editing, J.B., N.P., and V.P; All authors have read and agreed to the published version of the manuscript.

Acknowledgments

The authors would like to thank the trustees of Naran Lala College of Professional and Applied Sciences, Navsari, India, for their support and for providing resources to carry out this work.

Conflict of Interest

No conflict of interest

Ethical Approval

Not applicable

Funding

No external funding was received for this study

Data Availability

16s rRNA sequence of the potential isolate is available from NCBI and can be accessed at **https://www.ncbi.nlm.nih.gov/nuccore/2785060150.**

References

1. Abdelgalil SA, Soliman NA, Abo-Zaid GA, Abdel-Fattah YR (2022) Bioprocessing strategies for cost-effective large-scale production of bacterial laccase from Lysinibacillus macroides LSO using bio-waste. Int J Environ Sci Technol 19:1633–1652. https://doi.org/10.1007/s13762-021-03231-3
2. Abdulmumini SA, Lateef A, Gueguim-Kana EB, Beukes LS, Matyumza N (2025) Sustainable fungal production of pectinase in orange peel-based medium: Taguchi optimization, juice clarification and green synthesis of selenium nanoparticles for biomedical applications. Microbe 7:100400. https://doi.org/10.1016/j.microb.2025.100400
3. Ahamad Tarmizi AA, Nik Ramli NN, Adam SH, Abdul Mutalib M, Mokhtar MH, Tang SGH (2023) Phytofabrication of Selenium Nanoparticles with Moringa oleifera (MO-SeNPs) and Exploring Its Antioxidant and Antidiabetic Potential. Molecules 28:5322. https://doi.org/10.3390/molecules28145322
4. Alshammary M, Kotb E, Ababutain IM, Alabdalall AH, Aldakeel SA, Alsanie SI, Alhamad S, Alshwyeh H, Albarrag AM (2025) Production, Biochemical Characterization, and Application of Laccase from Halophilic Curvularia lunata MLK46 Recovered from Mangrove Rhizosphere. Biology 14:402. https://doi.org/10.3390/biology14040402
5. Arumugam DP, Uthandi S (2024) Optimization and characterization of laccase (LccH) produced by Hexagonia hirta MSF2 in solid-state fermentation using coir pith wastes (CPW). J Environ Manage 356:120625. https://doi.org/10.1016/j.jenvman.2024.120625
6. Baldrian P (2006) Fungal laccases – occurrence and properties. FEMS Microbiol Rev 30:215–242. https://doi.org/10.1111/j.1574-4976.2005.00010.x
7. Benavides V, Ciudad G, Pinto-Ibieta F, Robledo T, Rubilar O, Serrano A (2024) Enhancing Laccase and Manganese Peroxidase Activity in White-Rot Fungi: The Role of Copper, Manganese, and Lignocellulosic Substrates. Agronomy 14:2562. https://doi.org/10.3390/agronomy14112562
8. Bhatt P, Huang Y, Zhang W, Sharma A, Chen S (2020) Enhanced Cypermethrin Degradation Kinetics and Metabolic Pathway in Bacillus thuringiensis Strain SG4. Microorganisms 8, 223. https://doi.org/10.3390/microorganisms8020223
9. Bibi M, Yasmin A, Blanford C, Safdar N (2023) Production and characterization of a highly stable laccase from extreme thermophile *Geobacillus stearothermophilus* MB600 isolated from hot spring of Gilgit Balitistan (Pakistan). J Taibah Univ Sci 17:2268903. https://doi.org/10.1080/16583655.2023.2268903
10. Bisht N, Phalswal P, Khanna PK (2022) Selenium nanoparticles: a review on synthesis and biomedical applications. Mater Adv 3:1415–1431. https://doi.org/10.1039/D1MA00639H
11. Britos CN, Gianolini JE, Portillo H, Trelles JA (2018) Biodegradation of industrial dyes by a solvent, metal and surfactant-stable extracellular bacterial laccase. Biocatal Agric Biotechnol 14:221–227. https://doi.org/10.1016/j.bcab.2018.03.015
12. Chandel H, Yadav R, Shyam K, Sharma G, Murugesan S, Purchase D, Chaturvedi M, Saxena G (2026) Bioremediation of distillery effluent using a novel laccase-producing Bacillus velezensis HIM03: Process optimization, metabolite characterization, and phytotoxicity studies. J Environ Chem Eng 14:121943. https://doi.org/10.1016/j.jece.2026.121943
13. Colla IM, De O, Filho OBQ, Bertéli MBD, De Freitas JDS, Avelino KV, Ruiz SP, Do Valle JS, Linde GA, Colauto NB (2023) Carbon-to-nitrogen ratios on laccase and mushroom production of Lentinus crinitus. Int J Environ Sci Technol 20:3941–3952. https://doi.org/10.1007/s13762-022-04233-5
14. Cunningham TS, Andhare R, Cooper TG (2000) Nitrogen Catabolite Repression of DAL80Expression Depends on the Relative Levels of Gat1p and Ure2p Production in Saccharomyces cerevisiae. J Biol Chem 275:14408–14414.

https://doi.org/10.1074/jbc.275.19.14408

15. Das A, Sachdeva S, Jaswal V, Yogalakshmi KN (2022) Laccase Enzyme in Nanoparticle for Pesticide Degradation: A Special Emphasis on Chlorpyrifos Degradation. In: Singh VP, Yadav S, Yadav KK, Yadava RN (eds) Environmental Degradation: Challenges and Strategies for Mitigation, Water Science and Technology Library. Springer International Publishing, Cham, pp 345–369. https://doi.org/10.1007/978-3-030-95542-7_17
16. Deepa T, Gangwane AK, Sayyed RZ, Jadhav HP, Mehjabeen (2020) Optimization and scale-up of laccase production by Bacillus sp. BAB-4151 isolated from the waste of the soap industry. Environ Sustain 3:471–479. https://doi.org/10.1007/s42398-020-00135-9
17. El-Bendary MA, Ezzat SM, Ewais EA, Al-Zalama MA (2021) Optimization of spore laccase production by *Bacillus amyloliquefaciens* isolated from wastewater and its potential in green biodecolorization of synthetic textile dyes. Prep Biochem Biotechnol 51:16–27. https://doi.org/10.1080/10826068.2020.1786698
18. Elisashvili V, Penninckx M, Kachlishvili E, Tsiklauri N, Metreveli E, Kharziani T, Kvesitadze G (2008) Lentinus edodes and Pleurotus species lignocellulolytic enzymes activity in submerged and solid-state fermentation of lignocellulosic wastes of different composition. Bioresour Technol 99:457–462. https://doi.org/10.1016/j.biortech.2007.01.011
19. Elsayed AM, Mahmoud M, Abdel Karim GSA, Abdelraof M, Othman AM (2023) Purification and biochemical characterization of two laccase isoenzymes isolated from Trichoderma harzianum S7113 and its application for bisphenol A degradation. Microb Cell Factories 22:1. https://doi.org/10.1186/s12934-022-02011-z
20. Fahim YA, Ragab WM, Hasani IW, El-Khawaga AM (2025) Biomedical and environmental applications via nanobiocatalysts and enzyme immobilization. Eur J Med Res 30:505. https://doi.org/10.1186/s40001-025-02782-2
21. Frank JA, Reich CI, Sharma S, Weisbaum JS, Wilson BA, Olsen GJ (2008) Critical Evaluation of Two Primers Commonly Used for Amplification of Bacterial 16S rRNA Genes. Appl Environ Microbiol 74:2461–2470. https://doi.org/10.1128/AEM.02272-07
22. Garza-García JJO, Hernández-Díaz JA, León-Morales JM, Velázquez-Juárez G, Zamudio-Ojeda A, Arratia-Quijada J, Reyes-Maldonado OK, López-Velázquez JC, García-Morales S (2023) Selenium nanoparticles based on Amphipterygium glaucum extract with antibacterial, antioxidant, and plant biostimulant properties. J Nanobiotechnol 21:252. https://doi.org/10.1186/s12951-023-02027-6
23. Geng L, Li L, Sun X, Cheng S, He J (2025) Recent Advances Towards Selenium Nanoparticles: Synthetic Methods, Functional Mechanisms, and Biological Applications. Foods 14:3640. https://doi.org/10.3390/foods14213640
24. He J, Zhang K, Wang L, Du Y, Yang Y, Yuan C (2022) Highly efficient degradation of cypermethrin by a co-culture of Rhodococcus sp. JQ-L and Comamonas sp. A-3. Front Microbiol 13:1003820. https://doi.org/10.3389/fmicb.2022.1003820
25. Hosseini SM, Sepahi AA, Razavi MR, Saffarian P (2025) Optimizing Laccase Production From Halotolerant *Enterobacter* sp. *GR18* for Hydrocarbon Bioremediation. Remediat J 35:e70006. https://doi.org/10.1002/rem.70006
26. Huang Y, Xiao L, Li F, Xiao M, Lin D, Long X, Wu Z (2018) Microbial Degradation of Pesticide Residues and an Emphasis on the Degradation of Cypermethrin and 3-phenoxy Benzoic Acid: A Review. Molecules 23:2313. https://doi.org/10.3390/molecules23092313
27. Ibrahim SSS, Ansari YN, Puri AV, Patil VV, Gaikwad SS, Haroon RA (2024) Recent Progress in the Green Synthesis, Characterization, and Applications of Selenium Nanoparticles. BIO Integr 5. https://doi.org/10.15212/bioi-2024-0063
28. Illuri R, Kumar M, Eyini M, Veeramanikandan V, Almaary KS, Elbadawi YB, Biraqdar MA, Balaji P (2021) Production, partial purification and characterization of ligninolytic enzymes from selected basidiomycetes mushroom fungi. Saudi J Biol Sci 28:7207–7218. https://doi.org/10.1016/j.sjbs.2021.08.026
29. Jafari M, Mojtabavi S, Faramarzi MA, Mehrnejad F, Soleimani M, Mirjani R (2020) Molecular level insight into stability, activity, and structure of Laccase in aqueous ionic liquid and organic solvents: An experimental and computational research. J Mol Liq 317:113925. https://doi.org/10.1016/j.molliq.2020.113925
30. Janusz G, Pawlik A, Świderska-Burek U, Polak J, Sulej J, Jarosz-Wilkołazka A, Paszczyński A (2020) Laccase Properties, Physiological Functions, and Evolution. Int J Mol Sci 21:966. https://doi.org/10.3390/ijms21030966

31. Jones D n.d. Environmental Fate of Cypermethrin
32. Kansal I, Kapoor A, Solanki S, Singh R (2023) Cypermethrin toxicity in the environment: analytical insight into detection methods and microbial degradation pathways. J Appl Microbiol 134:lxad105. https://doi.org/10.1093/jambio/lxad105
33. Kasirajan L, Adams Z, Couto-Rodriguez RL, Gal D, Jia H, Mondragon P, Wassel PC, Yu D, Uthandi S, Maupin-Furlow JA (2021) High-level synthesis and secretion of laccase, a metalloenzyme biocatalyst, by the halophilic archaeon Haloferax volcanii. Methods Enzymol 659:297–313. https://doi.org/10.1016/bs.mie.2021.05.012
34. Kumar S, Saini P, Garla M (2025) Isolation, optimization, and characterization of laccase-producing bacteria for efficient lignin degradation. Bioresour Technol Rep 102382. https://doi.org/10.1016/j.biteb.2025.102382
35. Liu Q, Madadi M, Azad A, Sun S, Zhang C, Yan E, Samimi J, Sun A, F (2025) In-depth recognition of mixed surfactants maintaining the enzymatic activity of cellulases through stabilization of their spatial structures. Bioresour Technol 416:131756. https://doi.org/10.1016/j.biortech.2024.131756
36. Mahuri M, Paul M, Thatoi H (2023) A review of microbial laccase production and activity toward different biotechnological applications. Syst Microbiol Biomanufacturing 3:533–551. https://doi.org/10.1007/s43393-023-00163-6
37. Mate DM, Alcalde M (2015) Laccase engineering: From rational design to directed evolution. Biotechnol Adv 33:25–40. https://doi.org/10.1016/j.biotechadv.2014.12.007
38. Mehandia S, Sharma SC, Arya SK (2020) Isolation and characterization of an alkali and thermostable laccase from a novel Alcaligenes faecalis and its application in decolorization of synthetic dyes. Biotechnol Rep 25:e00413. https://doi.org/10.1016/j.btre.2019.e00413
39. Najafabadipour N, Mojtabavi S, Jafari-Nodoushan H, Samadi N, Faramarzi MA (2021) High efficiency of osmotically stable laccase for biotransformation and micro-detoxification of levofloxacin in the urea-containing solution: Catalytic performance and mechanism. Colloids Surf B Biointerfaces 207:112022. https://doi.org/10.1016/j.colsurfb.2021.112022
40. Nandal P, Ravella SR, Kuhad RC (2013) Laccase production by Coriolopsis caperata RCK2011: Optimization under solid state fermentation by Taguchi DOE methodology. Sci Rep 3:1386. https://doi.org/10.1038/srep01386
41. Oliveira TPDS, Lima AKO, Gonçalves TP, Florêncio I, Báo SN, Silva NOD, Albuquerque P, Silva-Pereira I, Muehlmann LA (2026) Synthesis of Selenium Nanoparticles: Influence of Reaction Parameters on Physicochemical, Morphological, and Biological Properties. Drugs Drug Candidates 5:22. https://doi.org/10.3390/ddc5010022
42. Orlando C, Rizzo IC, Arrigoni F, Zampolli J, Mangiagalli M, Di Gennaro P, Lotti M, De Gioia L, Marino T, Greco C, Bertini L (2024) Mechanism of non-phenolic substrate oxidation by the fungal laccase Type 1 copper site from *Trametes versicolor*: the case of benzo[*a*]pyrene and anthracene. Dalton Trans 53:12152–12161. https://doi.org/10.1039/D4DT01377H
43. Othman AM, Mahmoud M, Abdelraof M, Abdel Karim GSA, Elsayed AM (2021) Enhancement of laccase production from a newly isolated Trichoderma harzianum S7113 using submerged fermentation: Optimization of production medium via central composite design and its application for hydroquinone degradation. Int J Biol Macromol 192:219–231. https://doi.org/10.1016/j.ijbiomac.2021.09.207
44. Oyedeji BA, Oloye NR, Adebajo SO, Taiwo MO, Folarin BT, Akintokun AK (2025) Optimization and production of laccase enzyme by Bacillus cereus isolated from effluent of paint producing industry. Bull Natl Res Cent 49:27. https://doi.org/10.1186/s42269-025-01319-1
45. Parshad J, Kumar R, Kumar, Ajay, Chhokar V, Kumar A (2025) Intervention and Optimization of Urea (CH4N2O) for Enhancement of Lignocellulolytic Enzyme Production in Modified Potato Dextrose Media. Nat Environ Pollut Technol 24:B4299. https://doi.org/10.46488/NEPT.2025.v24i04.B4299
46. Pasinszki T, Krebsz M (2020) Synthesis and Application of Zero-Valent Iron Nanoparticles in Water Treatment, Environmental Remediation, Catalysis, and Their Biological Effects. Nanomaterials 10:917. https://doi.org/10.3390/nano10050917
47. Piscitelli A, Giardina P, Lettera V, Pezzella C, Sannia G, Faraco V (2011) Induction and Transcriptional Regulation of Laccases in Fungi. Curr Genomics 12:104–112. https://doi.org/10.2174/138920211795564331
48. Plackett RL, Burman JP (1946) THE DESIGN OF OPTIMUM MULTIFACTORIAL EXPERIMENTS. Biometrika 33:305–325. https://doi.org/10.1093/biomet/33.4.305

49. Rajendran S, Kalairaj A, Senthilvelan T (2025) A comprehensive review on enzymatic decolorization of various azo dyes using laccase for the abatement of industrial pollution. Biomass Convers Biorefinery 15:13079–13101. https://doi.org/10.1007/s13399-024-06104-0
50. Raturi P, Ahmad N, Rawat N, Singhvi N (2025) Synthesis and Biomedical Based Applications of Selenium Nanoparticles: A Comprehensive Review. Indian J Microbiol 65:204–215. https://doi.org/10.1007/s12088-024-01302-w
51. Rehman H, Rehman Z, Das TK, Rehman M, Khan BA, Nandi S, Ahmad K, Mohanty SK, Ur Rehman W, Naeem R, Bajaj M, Tuka MB (2024) Toxicity evaluation and degradation of cypermethrin-contaminated soil using biochar and Bacillus cereus amendments. Sci Rep 14:29892. https://doi.org/10.1038/s41598-024-81588-4
52. Ren S, Wang F, Gao H, Han X, Zhang T, Yuan Y, Zhou Z (2024) Recent Progress and Future Prospects of Laccase Immobilization on MOF Supports for Industrial Applications. Appl Biochem Biotechnol 196:1669–1684. https://doi.org/10.1007/s12010-023-04607-6
53. Shraddha, Shekher R, Sehgal S, Kamthania M, Kumar A (2011) Laccase: Microbial Sources, Production, Purification, and Potential Biotechnological Applications. Enzyme Res. 2011, 1–11. https://doi.org/10.4061/2011/217861
54. Stajic M, Persky L, Hadar Y, Friesem D, Duletic-Lausevic S, Wasser SP, Nevo E (2006) Effect of Copper and Manganese Ions on Activities of Laccase and Peroxidases in Three < I>Pleurotus Species Grown on Agricultural Wastes. Appl Biochem Biotechnol 128:087–096. https://doi.org/10.1385/ABAB:128:1:087
55. Sun K, Wu Z-H, Liu J, Cheng Z-H, Liu D-F, Lin H, Yu H-Q (2024) Unappreciated role of secondary metabolism-derived small mediators in degrading bisphenol A and antibiotics by a laccase-expressing fungus. Environ Pollut 363:125219. https://doi.org/10.1016/j.envpol.2024.125219
56. Tan WY, Gopinath SCB, Anbu P, Yaakub ARW, Subramaniam S, Chen Y, Sasidharan S (2023) Bio-Enzyme Hybrid with Nanomaterials: A Potential Cargo as Sustainable Biocatalyst. Sustainability 15:7511. https://doi.org/10.3390/su15097511
57. Tugarova AV, Mamchenkova PV, Dyatlova YA, Kamnev AA (2018) FTIR and Raman spectroscopic studies of selenium nanoparticles synthesised by the bacterium Azospirillum thiophilum. Spectrochim Acta Mol Biomol Spectrosc 192:458–463. https://doi.org/10.1016/j.saa.2017.11.050
58. Ullah A, Yin X, Wang F, Xu, Bo, Mirani ZA, Xu B, Chan MWH, Ali A, Usman M, Ali N, Naveed M (2021) Biosynthesis of Selenium Nanoparticles (via Bacillus subtilis BSN313), and Their Isolation, Characterization, and Bioactivities. Molecules 26:5559. https://doi.org/10.3390/molecules26185559
59. Vantamuri AB, Kaliwal BB (2016) Purification and characterization of laccase from Marasmius species BBKAV79 and effective decolorization of selected textile dyes. 3 Biotech 6:189. https://doi.org/10.1007/s13205-016-0504-9
60. Weisburg WG, Barns SM, Pelletier DA, Lane DJ (1991) 16S ribosomal DNA amplification for phylogenetic study. J Bacteriol 173:697–703. https://doi.org/10.1128/jb.173.2.697-703.1991
61. Wiśniewska KM, Twarda-Clapa A, Białkowska AM (2021) Screening of Novel Laccase Producers—Isolation and Characterization of Cold-Adapted Laccase from Kabatiella bupleuri G3 Capable of Synthetic Dye Decolorization. Biomolecules 11, 828. https://doi.org/10.3390/biom11060828
62. Xu R, Zhang X, Zelekew OA, Schott E, Wu Y (2023) Improved stability and activity of laccase through *de novo* and post-synthesis immobilization on a hierarchically porous metal–organic framework (ZIF-8). RSC Adv 13:17194–17201. https://doi.org/10.1039/D3RA01571H
63. Zhang J, Liu D, Liang X, Liu G, Wen C, Liang L, Liu X, Li Y, Xu X (2024) Synthesis and characterization of selenium nanoparticles stabilized by Grifola frondosa polysaccharides and gallic acid conjugates. Int J Biol Macromol 278:134787. https://doi.org/10.1016/j.ijbiomac.2024.134787
64. Zhao D, Yu S, Zang W, Ge J, Du R (2025) Exopolysaccharide-selenium composite nanoparticle: Characterization, antioxidant properties and selenium release kinetics in simulated gastrointestinal conditions. Int J Biol Macromol 304:140809. https://doi.org/10.1016/j.ijbiomac.2025.140809

Figures

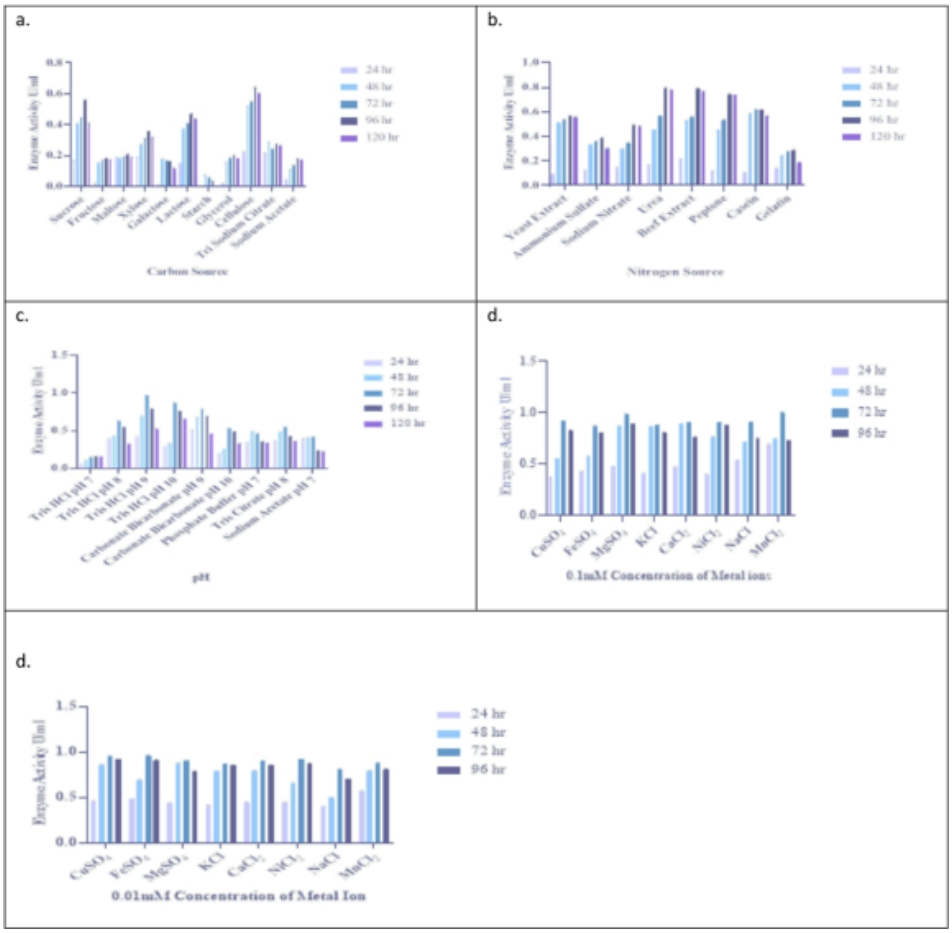


Figure 1

(a) Effect of various carbon sources, (b) nitrogen sources, (c) pH buffers, and (d) metal ion concentration (0.1mM and 0.01mM)

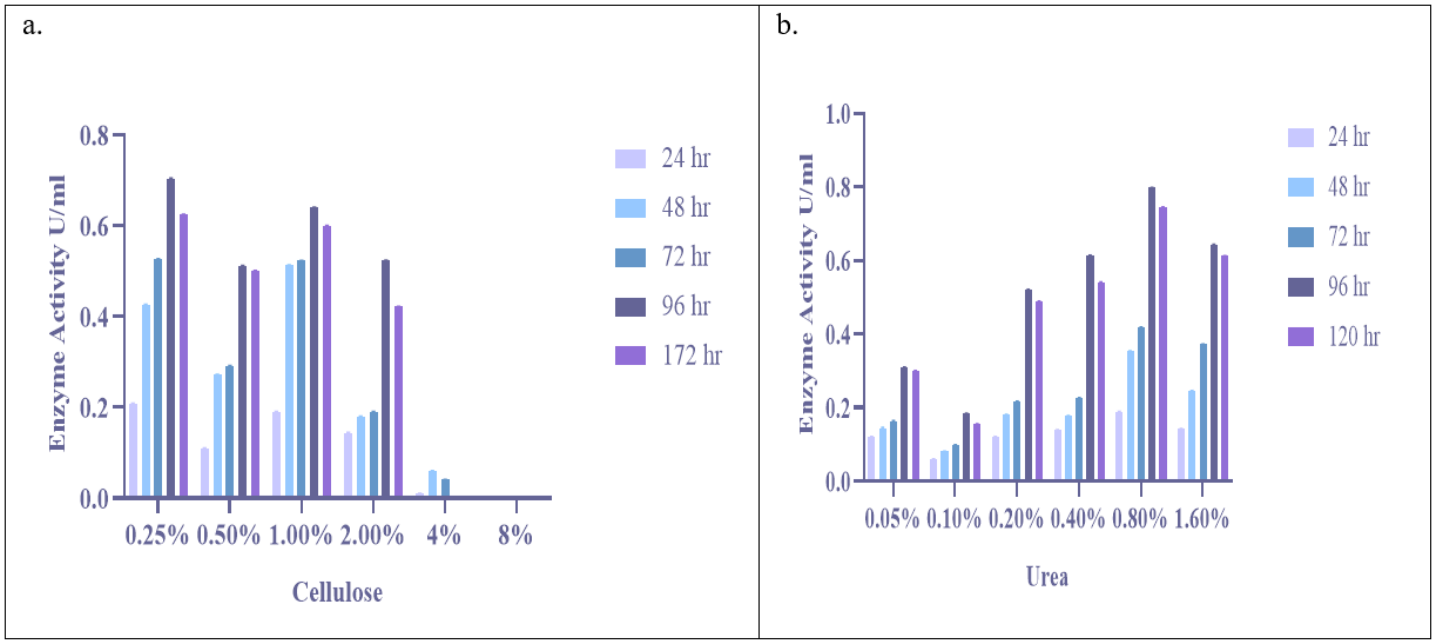


Figure 2

(a) Effect of Cellulose concentration and (b) Urea concentration

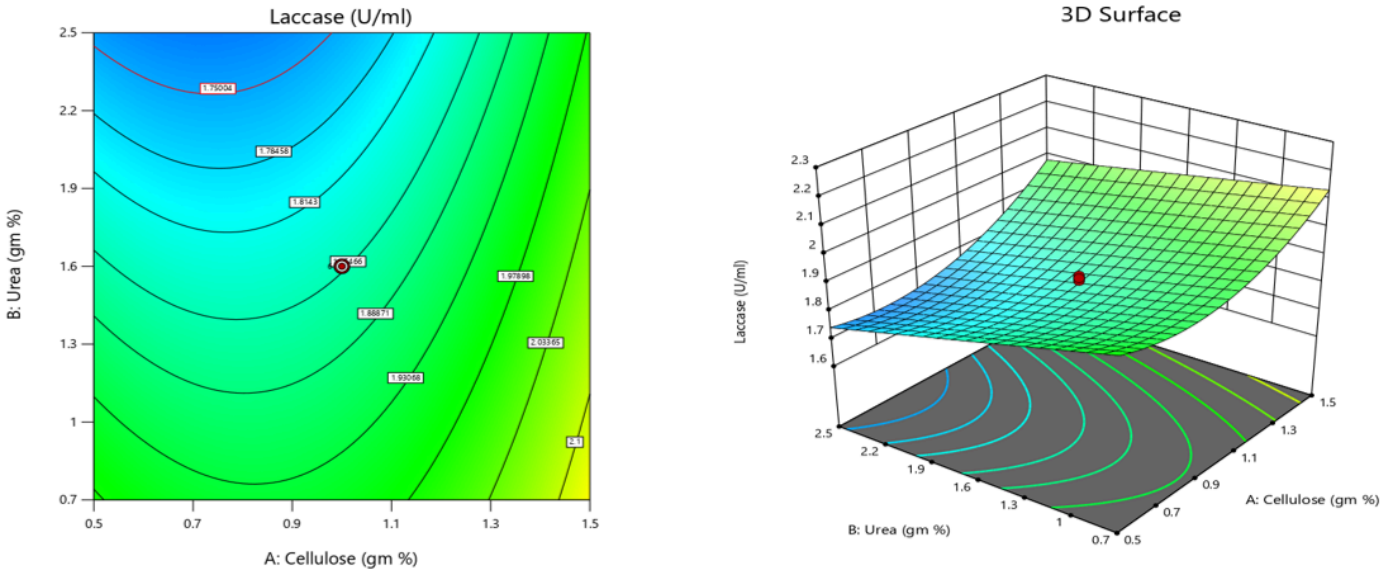


Figure 3

Response surface graph showing the interaction effect of cellulose and urea on laccase production

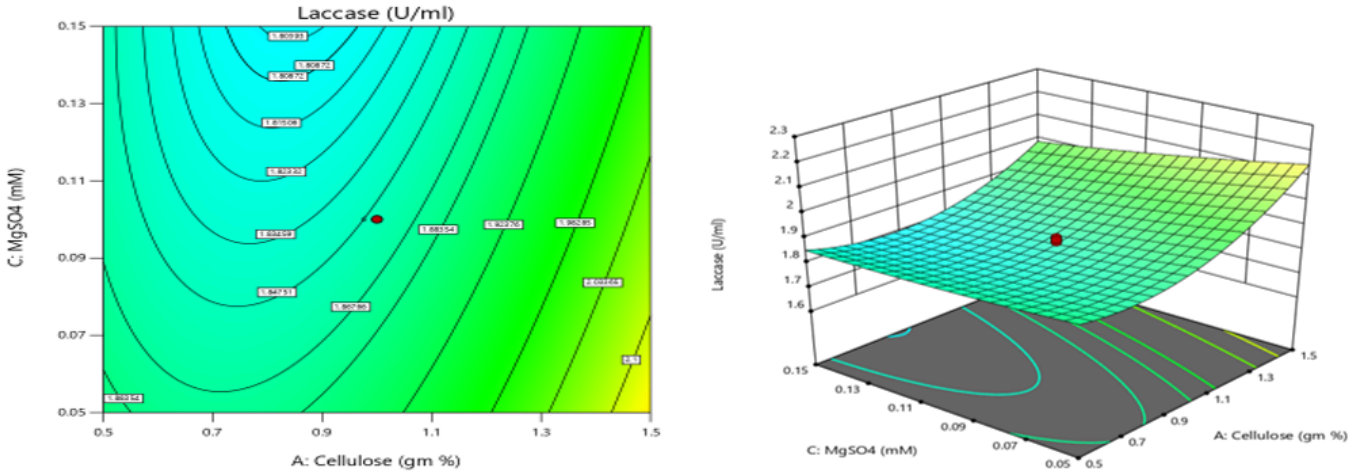


Figure 4

Response surface graph showing the interaction effect of cellulose and $MgSO_4$ on laccase production

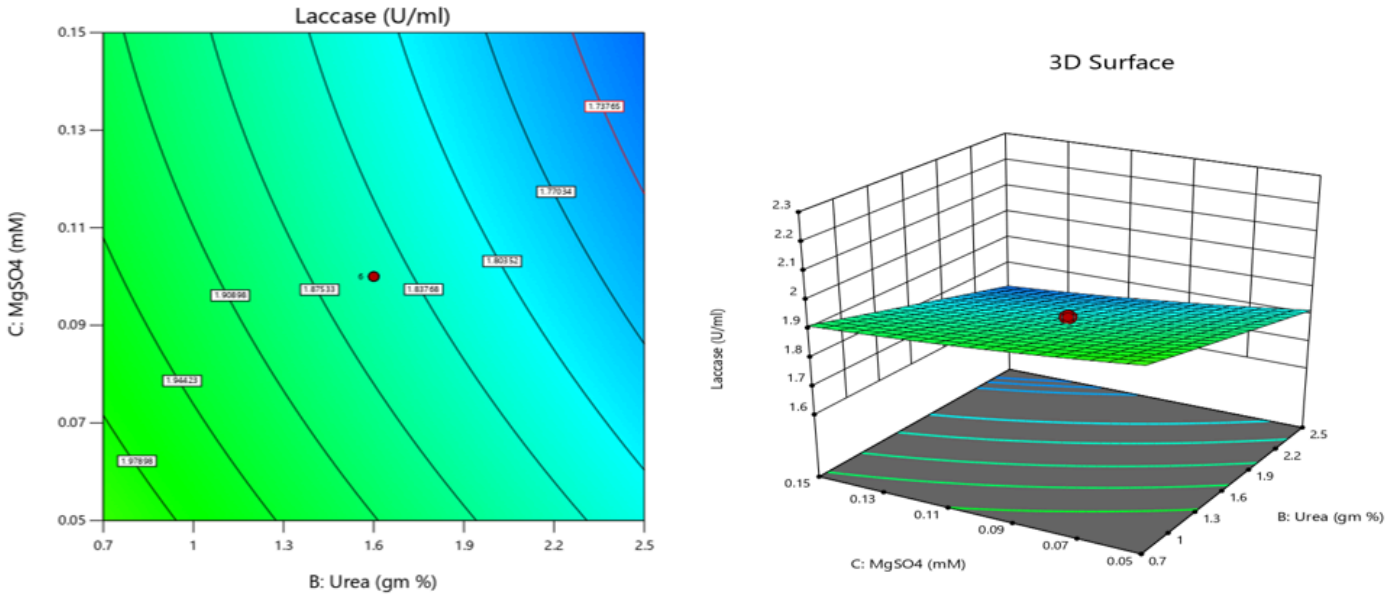


Figure 5

Response surface graph showing the interaction effect of urea and $MgSO_4$ on laccase production.

Supplementary Files

This is a list of supplementary files associated with this preprint. Click to download.

- Supplementaryfile.pdf